JMM

Targeted drug delivery in multi-layer capsules: an analytical and numerical study

Ebrahim Azhdari∗, **Aram Emami**

Department of Mathematics, Salman Farsi University of Kazerun, Fars, Kazerun, Iran
Email(s): e.azhdari@kazerunsfu.ac.ir, a.emami@kazerunsfu.ac.ir

Abstract. Recently, polymeric multi-layer capsules have gained a great deal of attention from the life science community. Furthermore, myriad interesting systems have appeared in the literature with biodegradable components and biospecific functionalities. In the present work, we presented a mathematical model of drug release from a multi-layer capsule into a target tissue. The diffusion problem was described by a system of coupled partial differential equations, Fickian and non-Fickian, which we solved numerically via nonuniform finite differences method. Energy estimates were further established for the coupled system and also, the convergence properties of the proposed numerical method were justified. We ultimately demonstrated the qualitative behavior of the system.

Keywords: Multi-layer capsules, drug release, viscoelastic, stability, convergence.
AMS Subject Classification 2010: 65M06.

1 Introduction

Capsules are currently utilized as targeted drug delivery systems to augment therapeutic efficacy and minimize the side effects. Capsules are composed of a drug-filled core surrounded by a few layers. These layers increase the mechanical stability of the capsule and prevent its degradation from the external chemical aggression [17, 21]. To surround the whole capsule structure, a thin layer is required so as to protect it from mechanical erosion and external chemical aggressions [14].

Some reviews have suggested models for drug release from coated formulations, polymeric materials, and capsules with empirical models [13, 20, 21]. There exists a mechanistic model for studying the drug release from a multi-layer coated spherical capsule [5, 15, 16]. In [16], the authors proposed a novel in silico model for computing drug release from multi-layer capsules. They delineated the diffusion issue in this heterogeneous layer-by-layer composite medium through a system of coupled partial differential equations and analytically solved the model by separating variables. In [5], the researchers made use

of the Laplace transform to solve the model. In [15], an alternative numerical approach was developed to investigate the mass transfer from a stationary core-shell reservoir under channel flow conditions. Using the lattice Boltzmann method, the author computed both the solvent fluid flow and the diffusion and advection of the solute. Pontrelli et al. [18] presented a mechanistic model of drug release from a multiple emulsion into an external surrounding fluid. Through the use of finite volume discretization, they solved the model numerically. In a majority of these investigations, the release and numerical behavior of drug were addressed whereas the viscoelasticity of the polymeric shell was neglected. This feature significantly affects the drug release scenario, hence the fact that it should be considered in the model.

The present research aimed to examine a system of one-dimensional coupled model that can be employed to elucidate the drug release from a drug-filled core to the polymeric shell with viscoelastic properties and its subsequent release into the target tissue. A non-Fickian mathematical model was presented for drug release in the polymeric shell. In this novel model, the Fick's law for the flux is modified through introducing a non-Fickian contribution defined with Maxwell fluid model [6, 7]. The coupled system is completed with initial, boundary, and interface conditions. We further established energy estimates for the coupled system based on [19]. These estimates were utilized to achieve an upper bound for the drug mass in the coupled system. Following [3, 10], we proposed a discrete model to numerically solve the coupled problem and demonstrate the qualitative behavior of the drug concentration in each layer. The accuracy of the spatial discretizations of the model was also determined.

The paper is organized as follows. Section 2 delineates the model and its initial, boundary, and interface conditions. Section 3 specifies the energy estimates for the coupled system. Section 4 introduces a numerical method that mimics the qualitative behavior of the continuous model. Numerical simulations are discussed in Section 5, and Section 6 concludes the paper.

2   Model development

Let us consider a multi-layer capsule made of an internal core or depot (Ω_0) surrounded by a number of layers (Ω_i, with $i = 1, \ldots, s$) as illustrated in Fig. 1. These layers are made of different materials, but homogeneous, and are controlling the drug release. The last outer shell is the target tissue. This layer can be considered as semi-infinite [5, 16]. Due to the homogeneity and isotropy of the layers, we can assume that drug penetration occurs only along the center line of the layers, and therefore we use a one-dimensional model for the study, which means $c_i(x, y, z, t) = c_i(x, 0, 0, t) = c_i(x, t)$, where c_i is the drug concentration of each layer. We consider the special case of the layers: a drug-filled core $\Omega_0 = (0, \ell_1)$, encapsulated by a single polymeric shell $\Omega_1 = (\ell_1, \ell_2)$ and surrounded by a target tissue $\Omega_2 = (\ell_2, \ell_3)$. We assume that $\ell_1 < \ell_2 < \ell_3$. Thus, the time-space drug evolution is described by the mass conservation law as following

$$\frac{\partial c_1}{\partial t} = D_1 \frac{\partial^2 c_1}{\partial x^2}, \ 0 < x < \ell_1, \tag{1}$$

$$\frac{\partial c_2}{\partial t} = D_2 \frac{\partial^2 c_2}{\partial x^2} + D_v \frac{\partial^2 \sigma}{\partial x^2}, \ \ell_1 < x < \ell_2, \tag{2}$$

$$\frac{\partial \sigma}{\partial t} + \frac{E}{\mu} \sigma = -\bar{E} c_2, \ \ell_1 < x < \ell_2, \tag{3}$$

$$\frac{\partial c_3}{\partial t} = D_3 \frac{\partial^2 c_3}{\partial x^2}, \ \ell_2 < x < \ell_3, \tag{4}$$

where D_i, $i = 1, 2, 3$ are the diffusion coefficients of the drug in the core, polymeric shell and target tissue,
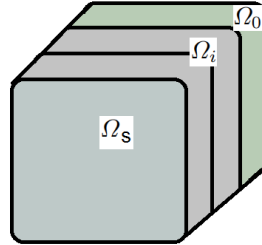
Figure 1: Drug releasing from a multi-layer capsule.

respectively, E represents the Young modulus of the material, μ is its viscosity, σ is the stress response to the strain and $\bar{E} = kE$, where k is a positive constant. Equations (1) and (4) are describing the distribution of the drug concentration in the drug-filled core and target tissue, respectively. Equation (2) is describing the distribution of the drug concentration in the polymeric shell which has viscoelastic properties. The viscoelastic influence in the drug transport is represented by the term $D_v \frac{\partial^2 \sigma}{\partial x^2}$ where D_v is the viscoelastic diffusion coefficient. The viscoelastic term states that the polymer acts as a barrier to the diffusion of the drug: as the drug strains the polymer it reacts with a stress of opposite sign [9]. Equation (3) defines the viscoelastic behavior of the polymer as described by the Maxwell fluid model [1, 2, 4, 6–8, 11, 12].

System (1)-(4) is complemented with the boundary conditions

$$\frac{\partial c_1}{\partial x}(0,t) = 0, \tag{5}$$

$$c_3(\ell_3, t) = 0, \tag{6}$$

interface conditions

$$-D_1 \frac{\partial c_1}{\partial x}(\ell_1, t) = -D_2 \frac{\partial c_2}{\partial x}(\ell_1, t) - D_v \frac{\partial \sigma}{\partial x}(\ell_1, t), \quad c_1(\ell_1, t) = \zeta c_2(\ell_1, t), \tag{7}$$

$$-D_2 \frac{\partial c_2}{\partial x}(\ell_2, t) - D_v \frac{\partial \sigma}{\partial x}(\ell_2, t) = -D_3 \frac{\partial c_3}{\partial x}(\ell_2, t) = P(c_2 - c_3), \tag{8}$$

and the initial condition

$$c_1(x,0) = C_0, \qquad c_2(x,0) = 0, \qquad c_3(x,0) = 0, \qquad \sigma(x,0) = \sigma_0. \tag{9}$$

Equation (5) means that the system is insulated while equation (6) states that the drug is immediately removed.

Equation (7) emphasises the continuity of the mass flux and the continuity of the concentration at the boundary between Ω_0 and Ω_1, where $\zeta = 1$ is a constant [10]. To help better control and prevent fast delivery, at the boundary between the polymer and the target tissue, Ω_1 and Ω_2, we assume the boundary is a thin layer with a small but not zero thickness. This assumed coating layer shields and preserves the encapsulated drug from degradation and fluid convection, protects the capsule structure and guarantees a more controlled and sustained release [16]. So the continuity of the mass flux and the continuity of the

concentration are then replaced with equation (8), where P is the shell mass transfer coefficient, which is a positive constant.

The initial condition means that there is initially a homogeneous drug distribution in the drug-filled core and that the polymeric shell and target tissue are empty. The C_0 is the initial concentration of drug and σ_0 is the initial stress.

The model which is presented by equations (1)-(9) can be used in drug delivery from multiple emulsions. The release of the drug from the nano-emojis means that the drug first enters the gel phase from the emulsion phase and then penetrates the target tissue from the gel phase.

3   Energy estimates

The qualitative behavior of the drug delivery in multi-layer capsules is studied through an a priori energy estimate. We show that the continuous model is stable, under initial perturbations, and for bounded intervals of time, by imposing some conditions on the parameters. These conditions appear as a technical tool, in the sense that they represent mathematical constraints needed to establish the result. They essentially say that the mathematical model is stable under some conditions. We introduce now the weak formulation of the initial-boundary value coupled problem (1)-(9). To do that we define the following spaces

$$V_i = \{w \in H^1(\ell_{i-1}, \ell_i) : w(\ell_3) = 0\},$$

for $i = 1, 2, 3$, where $\ell_0 = 0$. Let $(\cdot, \cdot)_i$ be the usual inner product in $L^2(\ell_{i-1}, \ell_i)$ and $\|\cdot\|_i$ the corresponding norm, $i = 1, 2, 3$, where $\ell_0 = 0$.

From equation (3) and by considering $c_2(x, 0) = 0$, we easily get

$$\sigma(x, t) = \bar{E} \int_0^t e^{-\frac{E}{\mu}(t-s)} c_2(s) ds + \sigma_0 e^{-\frac{E}{\mu}t}.$$

Using this equality in the equation (2) and considering σ_0 is a constant, we obtain for c_2 the following equation

$$\frac{\partial c_2}{\partial t} = D_2 \frac{\partial^2 c_2}{\partial x^2} + D_\sigma \int_0^t e^{-\frac{E}{\mu}(t-s)} \frac{\partial^2 c_2}{\partial x^2}(s) ds, \tag{10}$$

where $D_\sigma = \bar{E} D_v$. Then the interface boundary conditions (7) and (8) is replaced by the following interface boundary conditions

$$\begin{cases} -D_1 \dfrac{\partial c_1}{\partial x}(\ell_1, t) = -D_2 \dfrac{\partial c_2}{\partial x}(\ell_1, t) - D_\sigma \displaystyle\int_0^t e^{-\frac{E}{\mu}(t-s)} \dfrac{\partial c_2}{\partial x}(\ell_1, s) ds, \;\; c_1(\ell_1, t) = c_2(\ell_1, t), \\ -D_2 \dfrac{\partial c_2}{\partial x}(\ell_2, t) - D_\sigma \displaystyle\int_0^t e^{-\frac{E}{\mu}(t-s)} \dfrac{\partial c_2}{\partial x}(\ell_2, s) ds = -D_3 \dfrac{\partial c_3}{\partial x}(\ell_2, t) = P(c_2 - c_3). \end{cases} \tag{11}$$

The weak solution for the previous problem are functions $c_i \in L^2(\mathbb{R}^+, V_i) \cap C^1(\mathbb{R}^+, L^2(\ell_{i-1}, \ell_i))$, $i = 1, 2, 3$, $\ell_0 = 0$ such that

$$\sum_{i=1}^3 \left(\frac{\partial c_i}{\partial t}, w_i\right)_i = \sum_{i=1}^3 \left(D_i \frac{\partial^2 c_i}{\partial x^2}, w_i\right)_i + D_\sigma \int_0^t e^{-\frac{E}{\mu}(t-s)} \left(\frac{\partial^2 c_2}{\partial x^2}(s), w_2\right)_2 ds, \; w_i \in V_i, \tag{12}$$

for $i = 1, 2, 3$ and initial condition (9).

From (12), after replacing $w_i = c_i$, $i = 1, 2, 3$, we deduce

$$\sum_{i=1}^{3} \left(\frac{\partial c_i}{\partial t}, c_i \right)_i = \sum_{i=1}^{3} \left(D_i \frac{\partial^2 c_i}{\partial x^2}, c_i \right)_i + D_\sigma \int_0^t e^{-\frac{E}{\mu}(t-s)} \left(\frac{\partial^2 c_2}{\partial x^2}(s), c_2 \right)_2 ds, \tag{13}$$

Combining (13) with the boundary conditions (5) and (6) and the interface condition (11), we get

$$\frac{1}{2} \epsilon'(t) = -\sum_{i=1}^{3} D_i \left\| \frac{\partial c_i}{\partial x} \right\|_i^2 - D_\sigma \int_0^t e^{-\frac{E}{\mu}(t-s)} \left(\frac{\partial c_2}{\partial x}(s), \frac{\partial c_2}{\partial x} \right)_2 ds$$
$$- (P[c(t)], [c(t)])_{\ell_2}, \tag{14}$$

where $\epsilon(t) = \sum_{i=1}^{3} \|c_i(t)\|_i^2$ and

$$(P[c(t)], [c(t)])_{\ell_2} = \int_{\ell_2} P[c(t)]^2 d\mu,$$

$$[c(t)] = c_2(\ell_2, t) - c_3(\ell_2, t).$$

In what follows, we establish an estimate for the energy functional

$$\mathbb{E}(t) = \epsilon(t) + \sum_{i=1}^{3} \int_0^t \left\| \frac{\partial c_i}{\partial x}(s) \right\|_i^2 ds + \int_0^t \|[c(s)]\|_{\ell_2}^2 ds. \tag{15}$$

For any nonzero constant ε, we have the following inequality

$$D_\sigma \int_0^t e^{-\frac{E}{\mu}(t-s)} \left(\frac{\partial c_2}{\partial x}(s), \frac{\partial c_2}{\partial x} \right)_2 ds \leq \varepsilon^2 \left\| \frac{\partial c_2}{\partial x}(t) \right\|_2^2 + \frac{D_\sigma^2 \mu}{8\varepsilon^2 E} \int_0^t \left\| \frac{\partial c_2}{\partial x}(s) \right\|_2^2 ds. \tag{16}$$

Then, from (14) and using inequality (16), we get

$$\epsilon'(t) + 2 \sum_{i=1,3} D_i \left\| \frac{\partial c_i}{\partial x} \right\|_i^2 + 2(D_2 - \varepsilon^2) \left\| \frac{\partial c_2}{\partial x} \right\|_2^2 \leq \frac{D_\sigma^2 \mu}{4\varepsilon^2 E} \int_0^t \left\| \frac{\partial c_2}{\partial x}(s) \right\|_2^2 ds - 2P \|[c(t)]\|_{\ell_2}^2. \tag{17}$$

If we fix ε satisfying

$$D_2 - \varepsilon^2 > 0, \tag{18}$$

then

$$\epsilon(t) + 2 \sum_{i=1,3} D_i \int_0^t \left\| \frac{\partial c_i}{\partial x}(s) \right\|_i^2 ds + 2(D_2 - \varepsilon^2) \int_0^t \left\| \frac{\partial c_2}{\partial x}(s) \right\|_2^2 ds$$
$$\leq \frac{D_\sigma^2 \mu}{4\varepsilon^2 E} \int_0^t \int_0^v \left\| \frac{\partial c_2}{\partial x}(v) \right\|_2^2 dv ds - 2P \int_0^t \|[c(s)]\|_{\ell_2}^2 ds + \epsilon(0). \tag{19}$$

The equivalent of the above equation is as follows:

$$\mathbb{E}(t) \leq \Phi \int_0^t \mathbb{E}(s) ds + \epsilon(0), \tag{20}$$

where

$$\Phi = \frac{\min\{1, 2D_1, 2D_3, 2(D_2 - \varepsilon^2), 2P\}}{\frac{D_\sigma^2 \mu}{4\varepsilon^2 E}}. \tag{21}$$

By using Gronwall's Lemma we obtain the following result.

Theorem 1. *If $c_i \in L^2(\mathbb{R}^+, V_i) \cap C^1(\mathbb{R}^+, L^2(\ell_{i-1}, \ell_i))$, $i = 1, 2, 3$, $\ell_0 = 0$ are solutions of (12) and (9), then*

$$\mathbb{E}(t) \leq \epsilon(0)e^{\Phi t}, \tag{22}$$

where $D_2 - \varepsilon^2 > 0$ and Φ is defined by (21).

The upper bound (22) shows that the initial boundary value problem (1)-(9) is stable for bounded interval time that $D_2 - \varepsilon^2$ is positive.

The upper bound (22) can be used to describe the behavior of the coupled system for the drug mass of the coupled system. Let

$$M_i(t) = \int_{\ell_{i-1}}^{\ell_i} c_i(x,t)dx, \ i = 1,2,3, \ \ell_0 = 0, \ M(t) = \sum_{i=1}^{3} M_i(t) = \int_0^{\ell_3} c(x,t)dx, \tag{23}$$

be the mass in the layer $i, i = 1, 2, 3$ and the total mass, respectively. Using Hölder's inequality, we get

$$M^2(t) = \left(\int_0^{\ell_3} c(x,t)dx \right)^2 \leq \ell_3 \epsilon(t).$$

Hence, from equation (22), we get the following upper bound for the drug mass in the coupled system

$$M(t) \leq \sqrt{\ell_3 \epsilon(0)} e^{\frac{\Phi t}{2}}.$$

4   A discrete model

To simplify the equations, the following scaling groups are used, where the 'bar' corresponds to a non-dimensional variable,

$$\tau = \frac{D_{max} t}{\ell_3^2}, \ \xi = \frac{x}{\ell_3}, \ \bar{c}_i = \frac{c_i}{C_0}, \ \bar{\sigma} = \frac{\sigma}{\sigma_0}, \ \bar{D}_i = \frac{D_i}{D_{max}}, \ i = 1,2,3, \tag{24}$$

and $D_{max} = max\{D_i, i = 1, 2, 3\}$. Equations (1)-(9), after using (24), transform to

$$\frac{\partial \bar{c}_1}{\partial \tau} = \bar{D}_1 \frac{\partial^2 \bar{c}_1}{\partial \xi^2}, \qquad\qquad\qquad 0 < \xi < \frac{\ell_1}{\ell_3}, \tag{25}$$

$$\frac{\partial \bar{c}_2}{\partial \tau} = \bar{D}_2 \frac{\partial^2 \bar{c}_2}{\partial \xi^2} + D_{vnon} \frac{\partial^2 \bar{\sigma}}{\partial \xi^2}, \qquad \frac{\ell_1}{\ell_3} < \xi < \frac{\ell_2}{\ell_3}, \tag{26}$$

$$\frac{\partial \bar{\sigma}}{\partial \tau} + E_{non} \bar{\sigma} = -\mu_{non} \bar{c}_2, \qquad\quad \frac{\ell_1}{\ell_3} < \xi < \frac{\ell_2}{\ell_3}, \tag{27}$$

$$\frac{\partial \bar{c}_3}{\partial \tau} = \bar{D}_3 \frac{\partial^2 \bar{c}_3}{\partial \xi^2}, \qquad\qquad\qquad \frac{\ell_2}{\ell_3} < \xi < 1, \tag{28}$$
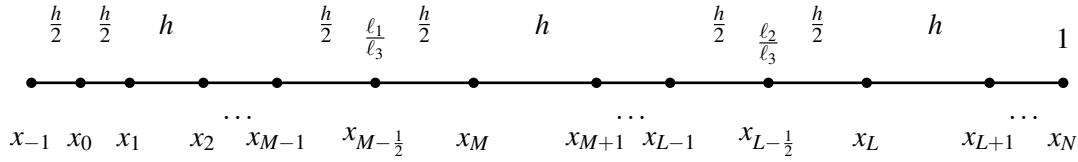
Figure 2: Schematic illustration of grid nodes in three layers.

$$\frac{\partial \bar{c}_1}{\partial \xi}(0, \tau) = 0, \tag{29}$$

$$\bar{c}_3(1, \tau) = 0, \tag{30}$$

$$-\bar{D}_1 \frac{\partial \bar{c}_1}{\partial \xi}\left(\frac{\ell_1}{\ell_3}, \tau\right) = -\bar{D}_2 \frac{\partial \bar{c}_2}{\partial \xi}\left(\frac{\ell_1}{\ell_3}, \tau\right) - D_{vnon} \frac{\partial \bar{\sigma}}{\partial \xi}\left(\frac{\ell_1}{\ell_3}, \tau\right), \quad \bar{c}_1\left(\frac{\ell_1}{\ell_3}, \tau\right) = \bar{c}_2\left(\frac{\ell_1}{\ell_3}, \tau\right) \tag{31}$$

$$-\bar{D}_2 \frac{\partial \bar{c}_2}{\partial \xi}\left(\frac{\ell_2}{\ell_3}, \tau\right) - D_{vnon} \frac{\partial \bar{\sigma}}{\partial \xi}\left(\frac{\ell_2}{\ell_3}, \tau\right) = -\bar{D}_3 \frac{\partial \bar{c}_3}{\partial \xi}\left(\frac{\ell_2}{\ell_3}, \tau\right) = \lambda (\bar{c}_2 - \bar{c}_3), \tag{32}$$

$$\bar{c}_1(\xi, 0) = 1, \qquad \bar{c}_2(\xi, 0) = 0, \qquad \bar{c}_3(\xi, 0) = 0, \qquad \bar{\sigma}(\xi, 0) = 1, \tag{33}$$

respectively, where several dimensionless controlling parameters are defined by

$$D_{vnon} = \frac{D_v \sigma_0}{D_{max} C_0}, E_{non} = \frac{E \ell_3^2}{D_{max} \mu}, \mu_{non} = \frac{\bar{E} C_0 \ell_3^2}{D_{max} \sigma_0}, \lambda = \frac{P \ell_3}{D_{max}}.$$

We introduce a discretization of the IBVP (25)-(33) which mimics its continuous counterpart. We fix a mesh size h. In the space domain $[0, 1]$, we introduce the grid $I_h = \{x_i, i = 0, \ldots, N\}$ as following (see Figure 2):

$$x_0 = 0, \ x_1 = x_0 + \frac{h}{2}, \ x_i = x_{i-1} + h, \ i = 2, \ldots, N, \ x_N = 1,$$

$$x_{M-\frac{1}{2}} = x_{M-1} + \frac{h}{2}, \ x_M = \frac{\ell_1}{\ell_3} + \frac{h}{2}, \ x_{L-\frac{1}{2}} = x_{L-1} + \frac{h}{2}, \ x_L = \frac{\ell_2}{\ell_3} + \frac{h}{2},$$

where $\frac{\ell_1}{\ell_3} = x_{M-\frac{1}{2}}$ and $\frac{\ell_2}{\ell_3} = x_{L-\frac{1}{2}}$. Let $x_{-1} = -\frac{h}{2}$ is the auxiliary point. By I_h^* we define the grid $I_h \cup \{x_{-1}\}$. By D_{-x}, D_x, D_c and $D_{2,h}$ we denote the backward, forward, first order centred and second order centred finite difference operators, respectively. We consider that $D_{2,h} v_h(x_{M-1})$ is based on a nonuniform grid and defined using the grid points x_{M-2}, x_{M-1} and $x_{M-\frac{1}{2}}$. Similarly, $D_{2,h} v_h(x_{L-1})$ is defined using the nonequally spaced grid points x_{L-2}, x_{L-1} and $x_{L-\frac{1}{2}}$.

Let $\bar{c}_h(\tau)$ and $\bar{\sigma}_h(\tau)$ be grid functions defined in the grid points $I_h^* \cup \{x_{M-\frac{1}{2}}, x_{L-\frac{1}{2}}\}$ that satisfies the following system of differential equations

$$\begin{cases} \bar{c}_i'(\tau) = \bar{D}_k D_{2,h} \bar{c}_i(\tau) + D_{vnon} D_{2,h} \bar{\sigma}_i(\tau), \\ \qquad i = 0, \ldots, M-1, M, M+1, \ldots, L-1, L, L+1, \ldots, N-1, \\ \bar{\sigma}_i'(\tau) + E_{non} \bar{\sigma}_i(\tau) = -\mu_{non} \bar{c}_i(\tau), \ i = M, \ldots, L-1, \end{cases} \tag{34}$$

where $\bar{D}_k = \bar{D}_1$, $D_{vnon} = 0$ if $i \leq M-1$, $\bar{D}_k = \bar{D}_2$, $D_{vnon} \neq 0$ if $M \leq i \leq L-1$ and $\bar{D}_k = \bar{D}_3$, $D_{vnon} = 0$ otherwise, coupled with the following algebraic conditions

$$\begin{cases} \bar{D}_1 D_c \bar{c}_0(\tau) = 0, \\ \bar{c}_N(\tau) = 0, \end{cases} \tag{35}$$

$$\begin{cases} -\bar{D}_1 D_{-x}\bar{c}_{M-\frac{1}{2}}(\tau) = -\bar{D}_2 D_x \bar{c}_{M-\frac{1}{2}}(\tau) - D_{vnon} D_x \bar{\sigma}_{M-\frac{1}{2}}(\tau), \\ -\bar{D}_2 D_{-x}\bar{c}_{L-\frac{1}{2}}(\tau) - D_{vnon} D_{-x}\bar{\sigma}_{L-\frac{1}{2}}(\tau) = -\bar{D}_3 D_x \bar{c}_{L-\frac{1}{2}}(\tau) = \lambda(\bar{c}_{L-1} - \bar{c}_L). \end{cases} \tag{36}$$

We assume that at the initial time we have

$$\bar{c}_i(0) = 1, \quad i = 0,\dots,M-1, \qquad \bar{c}_i(0) = 0, \quad i = M,\dots,N-1,$$
$$\bar{\sigma}_i(0) = 1, \quad i = M,\dots,L-1. \tag{37}$$

The boundary condition (35) and interface condition (36) are the discrete version of equations (29), (30) and (31), respectively.

Let us consider in the integration in time of the semi-discrete problem (34)-(37) the implicit-explicit method. To do that we fix a time interval $[0,T]$ where we introduce a time grid $\{\tau_n, \; n = 0,\dots, N_{\Delta\tau}\}$ in which $\tau_n - \tau_{n-1} = \Delta\tau, n = 1,\dots,N_{\Delta\tau}$, and $N_{\Delta\tau}\Delta\tau = T$. Let $\bar{c}_h^n, \bar{\sigma}_h^n, \; n = 0,\dots, N_{\Delta\tau}$ be defined by

$$\begin{cases} \bar{c}_i^{n+1} = \bar{c}_i^n + \Delta\tau \bar{D}_k D_{2,h}\bar{c}_i^{n+1} + \Delta\tau D_{vnon} D_{2,h}\bar{\sigma}_i^n, \\ \qquad i = 0,\dots, M-1, M, M+1,\dots, L-1, L, L+1,\dots, N-1, \\ \bar{\sigma}_i^{n+1} + (\Delta\tau E_{non} - 1)\bar{\sigma}_i^n = -\Delta\tau\mu_{non}\bar{c}_i^{n+1}, \quad i = M,\dots, L-1, \end{cases} \tag{38}$$

where $n = 0,\dots, N_{\Delta\tau} - 1$ and $\bar{D}_k = \bar{D}_1$, $D_{vnon} = 0$ if $i \leq M-1$, $\bar{D}_k = \bar{D}_2$, $D_{vnon} \neq 0$ if $M \leq i \leq L-1$, $\bar{D}_k = \bar{D}_3$, $D_{vnon} = 0$, otherwise,

$$\begin{cases} \bar{D}_1 D_c \bar{c}_0^n = 0, & n = 0,\dots, N_{\Delta\tau}, \\ \bar{c}_N^n = 0, & n = 1,\dots, N_{\Delta\tau}, \end{cases} \tag{39}$$

$$\begin{cases} -\bar{D}_1 D_{-x}\bar{c}_{M-\frac{1}{2}}^n = -\bar{D}_2 D_x \bar{c}_{M-\frac{1}{2}}^n - D_{vnon} D_x \bar{\sigma}_{M-\frac{1}{2}}^n, & n = 1,\dots, N_{\Delta\tau}, \\ -\bar{D}_2 D_{-x}\bar{c}_{L-\frac{1}{2}}^n - D_{vnon} D_{-x}\bar{\sigma}_{L-\frac{1}{2}}^n = -\bar{D}_3 D_x \bar{c}_{L-\frac{1}{2}}^n = \lambda(\bar{c}_{L-1}^n - \bar{c}_L^n). \end{cases} \tag{40}$$

We assume that at the initial time we have

$$\bar{c}_i^0 = 1, \quad i = 0,\dots,M-1, \qquad \bar{c}_i^0 = 0, \quad i = M,\dots,N-1,$$
$$\bar{\sigma}_i^0 = 1, \quad i = M,\dots,L-1. \tag{41}$$

4.1 Error analysis

To justify the behavior of the numerical method (38)-(41), in what follows we study the spatial discretization considering only the drug concentration, after solving the equation (27) and replacing in the

equation (26). In this scenario, we analyze the convergence behavior of the solution of the differential problem

$$\frac{d\bar{c}_h}{d\tau}(x_i, \tau) = \bar{D}_k D_{2,h}\bar{c}_h(\tau) - \mu_{non}D_{vnon}\int_0^\tau e^{-E_{non}(\tau-s)}D_{2,h}\bar{c}_h(s)ds,$$

$$i = 0,\ldots, M-1, M, M+1,\ldots, L-1, L, L+1,\ldots, N-1, \tag{42}$$

where $\bar{D}_k = \bar{D}_1$, $D_{vnon} = 0$, if $i \le M-1$, $\bar{D}_k = \bar{D}_2$, $D_{vnon} \ne 0$, if $M \le i \le L-1$ and $\bar{D}_k = \bar{D}_3$, $D_{vnon} = 0$, otherwise,

$$\begin{cases} D_c\bar{c}_h(x_0, \tau) = 0, \\ \bar{c}_h(x_N, \tau) = 0, \end{cases} \tag{43}$$

$$\begin{cases} -\bar{D}_1 D_{-x}\bar{c}_h(x_{M-\frac{1}{2}}, \tau) = -\bar{D}_2 D_x\bar{c}_h(x_{M-\frac{1}{2}}, \tau) + D_{vnon}\mu_{non}\int_0^\tau e^{-E_{non}(\tau-s)}D_x\bar{c}_h(x_{M-\frac{1}{2}}, s)ds, \\ -\bar{D}_2 D_{-x}\bar{c}_h(x_{L-\frac{1}{2}}, \tau) + D_{vnon}\mu_{non}\int_0^\tau e^{-E_{non}(\tau-s)}D_{-x}\bar{c}_h(x_{L-\frac{1}{2}}, s)ds \\ \qquad = -\bar{D}_3 D_x\bar{c}_h(x_{L-\frac{1}{2}}, \tau) = \lambda\left(\bar{c}_h(x_{L-1}, \tau) - \bar{c}_h(x_L, \tau)\right). \end{cases} \tag{44}$$

We assume that at the initial time we have

$$\bar{c}_h(0) = 1. \tag{45}$$

Let $E_h(\tau) = R_h\bar{c}(\tau) - \bar{c}_h(\tau)$ be the semi-discretization error induced by the spatial discretizations (42)-(45), where R_h is the restriction operator and let $T_h(\tau)$ be the corresponding truncation error. We have

$$\frac{dE_h}{d\tau}(x_i, \tau) = \bar{D}_k D_{2,h}E_h(\tau) - \mu_{non}D_{vnon}\int_0^\tau e^{-E_{non}(\tau-s)}D_{2,h}E_h(s)ds + T_h(x_i, \tau),$$

$$i = 0,\ldots, M-1, M, M+1,\ldots, L-1, L, L+1,\ldots, N-1, \tag{46}$$

where $\bar{D}_k = \bar{D}_1$, $D_{vnon} = 0$, if $i \le M-1$, $\bar{D}_k = \bar{D}_2$, $D_{vnon} \ne 0$, if $M \le i \le L-1$ and $\bar{D}_k = \bar{D}_3$, $D_{vnon} = 0$ otherwise,

$$\begin{cases} D_c E_h(x_0, \tau) = T_{lef}(\tau), \\ E_h(x_N, \tau) = 0, \end{cases} \tag{47}$$

$$\begin{cases} -\bar{D}_1 D_{-x}E_h(x_{M-\frac{1}{2}}, \tau) = -\bar{D}_2 D_x E_h(x_{M-\frac{1}{2}}, \tau) \\ \qquad\qquad +D_{vnon}\mu_{non}\int_0^\tau e^{-E_{non}(\tau-s)}D_x E_h(x_{M-\frac{1}{2}}, s)ds + T_{int,lef}(\tau), \\ -\bar{D}_2 D_{-x}E_h(x_{L-\frac{1}{2}}, \tau) + D_{vnon}\mu_{non}\int_0^\tau e^{-E_{non}(\tau-s)}D_{-x}E_h(x_{L-\frac{1}{2}}, s)ds \\ \qquad = -\bar{D}_3 D_x E_h(x_{L-\frac{1}{2}}, \tau) = \lambda\left(E_h(x_{L-1}, \tau) - E_h(x_L, \tau)\right) + T_{int,rig}(\tau), \end{cases} \tag{48}$$

where $T_{lef}(\tau)$, $T_{int,lef}(\tau)$ and $T_{int,rig}(\tau)$ are the truncation errors in x_0, $x_{M-\frac{1}{2}}$ and $x_{L-\frac{1}{2}}$, respectively.

We assume that at the initial time we have

$$E_h(0) = 0. \tag{49}$$

If we assume that $\bar{c}(\tau) \in C^4([\frac{-h}{2}, 1])$, then $\|T_h(\tau)\|_\infty \leq Ch^2$.

We introduce the following discrete $L^2(0,1)$ inner product $(.,.)_h$ for grid functions defined in I_h and null on x_N,

$$
(u_h, v_h)_h = \frac{h}{4} u_0 v_0 + \sum_{j=1}^{M-2} h u_j v_j + \frac{3}{4} h (u_{M-1} v_{M-1} + u_M v_M)
$$
$$
+ \sum_{j=M+1}^{L-2} h u_j v_j + \frac{3}{4} h (u_{L-1} v_{L-1} + u_L v_L) + \sum_{j=L+1}^{N-1} h u_j v_j.
$$

By $\|\cdot\|_h$, we denote the norm induced by this inner product. For grid functions defined in $I_h \cup \{x_{M-\frac{1}{2}}, x_{L-\frac{1}{2}}\}$ we use the following notations

$$
(u_h, v_h)_+ = \frac{h}{2} u_1 v_1 + \sum_{j=2}^{M-1} h u_j v_j + \frac{h}{2} (u_{M-\frac{1}{2}} v_{M-\frac{1}{2}} + u_M v_M)
$$
$$
+ \sum_{j=M+1}^{L-1} h u_j v_j + \frac{h}{2} (u_{L-\frac{1}{2}} v_{L-\frac{1}{2}} + u_L v_L) + \sum_{j=L+1}^{N} h u_j v_j,
$$

and

$$\|v_h\|_+ = (v_h, v_h)_+^{\frac{1}{2}}.$$

Theorem 2. *Let u_h, v_h be grid functions defined in $\bar{I}_h \cup \{x_{-\frac{h}{2}}, x_M, x_L\}$. Then*

$$
\begin{aligned}
(D_{2,h} u_h, v_h)_h = &- D_c u_h(x_0) v_h(x_0) - (D_{-x} u_h, D_{-x} v_h)_+ \\
&+ D_{-x} u_h(x_{M-\frac{1}{2}}) v_h(x_{M-\frac{1}{2}}) - D_x u_h(x_{M-\frac{1}{2}}) v_h(x_{M-\frac{1}{2}}) \\
&- (D_{-x} u_h, D_{-x} v_h)_+ + D_{-x} u_h(x_{L-\frac{1}{2}}) v_h(x_{L-\frac{1}{2}}) \\
&- D_x u_h(x_{L-\frac{1}{2}}) v_h(x_{L-\frac{1}{2}}) - (D_{-x} u_h, D_{-x} v_h)_+ \\
&+ D_c u_h(x_N) v_h(x_N).
\end{aligned}
$$

Theorem 3. *If $\bar{c} \in C^4([-\frac{h}{2}, 1])$, then the error $E_h(\tau)$ satisfies the following*

$$
\|E_h(\tau)\|_h^2 + 2 \left(\sum_{i=1}^{3} \bar{D}_i - \varepsilon^2 - \eta - (1+\lambda) \frac{\ell_3^2}{2} - \frac{D_{vnon}^2 \mu_{non}^2}{4\varepsilon^2 E_{non}} \right) \int_0^\tau \|D_{-x} E_h(s)\|_+^2 ds
$$
$$
\leq \int_0^\tau g_h(s) ds, \tag{50}
$$

where ε, η and λ are nonzero constants and

$$g_h(s) = \|T_h(s)\|_h^2 + T_{lef}(s)^2 + T_{int,lef}(s)^2 + T_{int,rig}(s)^2.$$

Proof. From the differential equation of (46), we get

$$\frac{1}{2}\frac{d}{d\tau}\|E_h(\tau)\|_h^2 = (\bar{D}_k D_{2,h}E_h(\tau), E_h(\tau))_h - D_{vnon}\mu_{non}\int_0^\tau e^{-E_{non}(\tau-s)}(D_{2,h}E_h(s), E_h(\tau))_h ds$$
$$+ (T_h(t), E_h(\tau))_h. \tag{51}$$

From Theorem 2 and (51), we get

$$\frac{1}{2}\frac{d}{d\tau}\|E_h(\tau)\|_h^2 = -\bar{D}_1 D_c E_h(x_0)E_h(x_0) - (\bar{D}_1 D_{-x}E_h(\tau), D_{-x}E_h(\tau))_+$$
$$+ \bar{D}_1 D_{-x}E_h(x_{M-\frac{1}{2}})E_h(x_{M-\frac{1}{2}}) - \bar{D}_2 D_x E_h(x_{M-\frac{1}{2}})E_h(x_{M-\frac{1}{2}})$$
$$+ D_{vnon}\mu_{non}\int_0^\tau e^{-E_{non}(\tau-s)}D_x E_h(x_{M-\frac{1}{2}})ds E_h(x_{M-\frac{1}{2}})$$
$$- (\bar{D}_2 D_{-x}E_h(\tau), D_{-x}E_h(\tau))_+$$
$$+ D_{vnon}\mu_{non}\int_0^\tau e^{-E_{non}(\tau-s)}(D_{-x}E_h(s), D_{-x}E_h(\tau))_+ ds$$
$$+ \bar{D}_2 D_{-x}E_h(x_{L-\frac{1}{2}})E_h(x_{L-\frac{1}{2}})$$
$$- D_{vnon}\mu_{non}\int_0^\tau e^{-E_{non}(\tau-s)}D_{-x}E_h(x_{L-\frac{1}{2}})ds E_h(x_{L-\frac{1}{2}})$$
$$- \bar{D}_3 D_x E_h(x_{L-\frac{1}{2}})E_h(x_{L-\frac{1}{2}}) - (\bar{D}_3 D_{-x}E_h(\tau), D_{-x}E_h(\tau))_+$$
$$+ \bar{D}_3 D_c E_h(x_N)E_h(x_N) + (T_h(\tau), E_h(\tau))_h. \tag{52}$$

Taking equations (47) and (48) in (52) we deduce that

$$\frac{1}{2}\frac{d}{d\tau}\|E_h(\tau)\|_h^2 = -T_{lef}(\tau)E_h(x_0) - \bar{D}_1\|D_{-x}E_h(\tau)\|_+^2$$
$$- T_{int,lef}(\tau)E_h(x_{M-\frac{1}{2}}) - \bar{D}_2\|D_{-x}E_h(\tau)\|_+^2$$
$$+ D_{vnon}\mu_{non}\int_0^\tau e^{-E_{non}(\tau-s)}(D_{-x}E_h(s), D_{-x}E_h(\tau))_+ ds$$
$$- \left(T_{int,rig} + P(E_h(x_{L-1}, \tau) - E_h(x_L, \tau))\right)E_h(x_{L-\frac{1}{2}})$$
$$- \bar{D}_3\|D_{-x}E_h(\tau)\|_+^2 + (T_h(\tau), E_h(\tau))_h. \tag{53}$$

Using

$$\int_0^\tau e^{-E_{non}(\tau-s)}ds = \frac{1}{E_{non}}(1 - e^{-E_{non}}) \le \frac{1}{E_{non}}, \tag{54}$$

and the CauchySchwarz inequality, we get

$$D_{vnon}\mu_{non}\int_0^\tau e^{-E_{non}(\tau-s)}(D_{-x}E_h(s), D_{-x}E_h(\tau))_+ ds$$
$$\le \frac{D_{vnon}^2\mu_{non}^2}{4\varepsilon^2}\int_0^\tau e^{-E_{non}(\tau-s)}e^{-E_{non}(\tau-s)}\|D_{-x}E_h(s)\|_+^2 ds + \varepsilon^2\|D_{-x}E_h(\tau)\|_+^2$$
$$\le \frac{D_{vnon}^2\mu_{non}^2}{4\varepsilon^2 E_{non}}\int_0^\tau e^{-E_{non}(\tau-s)}\|D_{-x}E_h(s)\|_+^2 ds + \varepsilon^2\|D_{-x}E_h(\tau)\|_+^2. \tag{55}$$

Taking in (53), the estimates (55) and using CauchySchwarz inequality and the equality

$$E_h(x_{\alpha-\frac{1}{2}}) = \frac{h}{2}D_{-x}E_h(x_{\alpha-\frac{1}{2}}) + E_h(x_{\alpha-1}), \quad \alpha = M, L, \tag{56}$$

we obtain

$$\frac{d}{d\tau}\|E_h(\tau)\|_h^2 + 2\Big(\sum_{i=1}^{3}\bar{D}_i - \varepsilon^2 - \eta\Big)\|D_{-x}E_h(\tau)\|_+^2$$

$$\leq \|T_h(\tau)\|_h^2 + (1+\lambda)\|E_h(\tau)\|_h^2 + \frac{D_{vnon}^2\mu_{non}^2}{2\varepsilon^2 E_{non}}\int_0^\tau e^{-E_{non}(\tau-s)}\|D_{-x}E_h(s)\|_+^2 ds + T_{lef}(\tau)^2$$

$$+ T_{int,lef}(\tau)^2 + T_{int,rig}(\tau)^2.$$

From Theorem 2 in [10], we know

$$\|E_h\|_h^2 \leq \ell_3^2\|D_{-x}E_h\|_+^2. \tag{57}$$

By integrating with respect to time and using (57), we obtain

$$\|E_h(\tau)\|_h^2 + 2\Big(\sum_{i=1}^{3}\bar{D}_i - \varepsilon^2 - \eta - (1+\lambda)\frac{\ell_3^2}{2}\Big)\int_0^\tau \|D_{-x}E_h(s)\|_+^2 ds$$

$$\leq \int_0^\tau g_h(s)ds + \frac{D_{vnon}^2\mu_{non}^2}{2\varepsilon^2 E_{non}}\int_0^\tau\int_0^\gamma e^{-E_{non}(\gamma-s)}\|D_{-x}E_h(s)\|_+^2 d\gamma ds.$$

Changing the order of integration in the double integral and using (54) we have

$$\|E_h(\tau)\|_h^2 + 2\Big(\sum_{i=1}^{3}\bar{D}_i - \varepsilon^2 - \eta - (1+\lambda)\frac{\ell_3^2}{2}\Big)\int_0^\tau \|D_{-x}E_h(s)\|_+^2 ds$$

$$\leq \int_0^\tau g_h(s)ds + \frac{D_{vnon}^2\mu_{non}^2}{2\varepsilon^2 E_{non}}\int_0^\tau\int_s^\tau e^{-E_{non}(\gamma-s)}d\gamma\|D_{-x}E_h(s)\|_+^2 ds$$

$$\leq \int_0^\tau g_h(s)ds + \frac{D_{vnon}^2\mu_{non}^2}{2\varepsilon^2 E_{non}^2}\int_0^\tau \|D_{-x}E_h(s)\|_+^2 ds. \tag{58}$$

Finally, we obtain (50).   □

Corollary 1. *Under the assumptions of Theorem 3, there exist a positive constant C, h and τ-independent, such that*

$$\|E_h(\tau)\|_h^2 + \int_0^\tau \|D_{-x}E_h(s)\|_+^2 ds \leq Ch^4, \tau \in [0,T]. \tag{59}$$

5 Numerical simulations and discussions

Here we illustrate the qualitative behavior of the (25)-(33) using the method (38)-(41) for the parameters listed as following [5, 16]:

$$\ell_1 = 1.5 \times 10^{-3}m, \ \ell_2 = 1.8 \times 10^{-3}m, \ \ell_3 = 3 \times 10^{-2}m,$$

$$D_1 = 3 \times 10^{-10}\frac{m^2}{s}, \ D_2 = 5 \times 10^{-11}\frac{m^2}{s}, \ D_3 = 3 \times 10^{-10}\frac{m^2}{s},$$

Table 1: Convergence rates $p(c)$

h	$E_{h,c}$	$p(c)$
0.05	8.6342×10^{-3}	1.77
0.01	5.0292×10^{-4}	1.86
0.005	1.3882×10^{-4}	2.01
0.002	2.1946×10^{-5}	——

$$P = 1 \times 10^{-8} \frac{m}{s}, \; D_v = 4 \times 10^{-12} \frac{mol}{m.s.Pa}, \; E = 5 \times 10^3 Pa,$$

$$\mu = 5 \times 10^9 Pa.s, \; C_0 = 1 \frac{mol}{m^3}, \; \sigma_0 = 2 \times 10^{-2} Pa,$$

$$k = 1 \times 10^{-12} \frac{m^3}{mol.s}, \; h = 1 \times 10^{-2} m, \; \Delta t = 2 \times 10^{-7} s.$$

In what follows, we illustrate Corollary 1. We present the convergence rates in Table 1 as following

$$p(c) = \frac{\ln \left(\frac{E_{h_1,c}}{E_{h_2,c}} \right)}{\ln \left(\frac{h_1}{h_2} \right)},$$

where $E_{h,c}$ is defined by

$$E_{h,c} = \max_{n=1,\dots,M} \left(\|E_h^n\|_h^2 + \Delta t \sum_{j=1}^n \|D_{-x} E_h^j\|_+^2 \right)^{\frac{1}{2}}.$$

These convergence rates were obtained for the numerical approximations computed with the method (38)-(41) for equations (25)-(33) and the reference solution defined by $h = 0.001$ and $\Delta t = 2 \times 10^{-7}$.

The numerical estimates for the rate of convergence presented in Table 1 confirms the theoretical estimate given in Corollary 1 which is second order approximation, $E_{h,c} = O(h^2)$.

Via the polymeric shell, the drug was transported from the inner core, to the target tissue. Each layer received mass from the previous layer and transferred it to the next layer until a complete drug release from the capsule. Figure 3 depicts the concentration profiles related to different P values at different times. With the increase in time, the concentration decreased inside each layer. Concerning small P, the interface between polymeric shell and target tissue acted as an impermeable barrier with a significantly low transfer rate from the capsule to the target tissue. The increase in the P value had a major impact on the release rate, reduced the drug concentration in the core, and increased it in the target tissue.

Figure 4 illustrates that the drug mass, defined as (23) for each layer, was monotonically reduced in the core, while at the same time increasing up to some peak before decaying asymptotically in the polymeric shell layer. In the target tissue, the mass progressively increased at a rate which depended on the diffusive properties of the layers. It can be observed that the core was completely emptied following the increase in P, at which point, all the mass was transferred to the target tissue. In terms of small P, it was found that plenty of drug mass remained in the core and less drug was released into the target tissue.
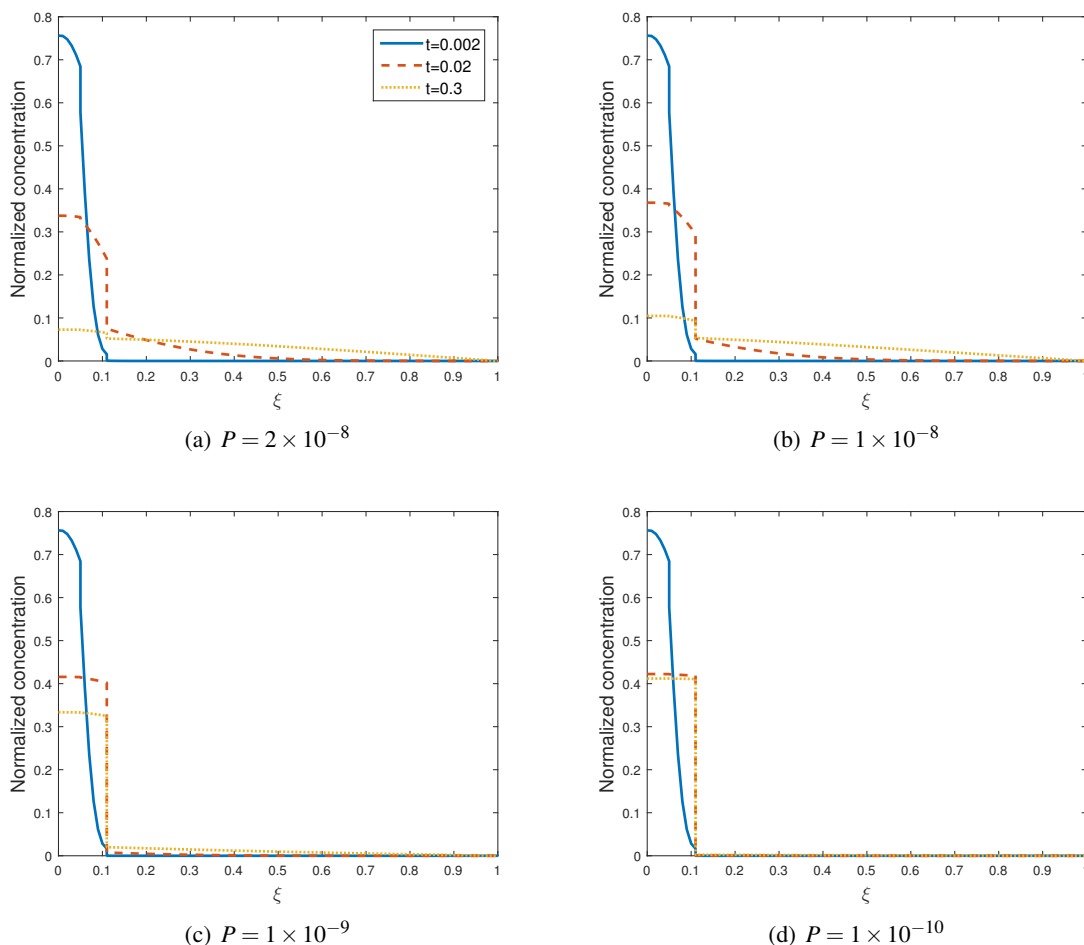
Figure 3: Normalized concentration profiles in the three layers.

Table 2 presents a number of simulations, clarifying the effect of the mechanical behavior of the polymeric shell on drug release concentration. When viscoelasticity was considered (for different values of D_v), the polymeric shell acted as a barrier against the drug release into the polymeric shell from the drug-filled core, reducing the drug release into the target tissue. This table also shows the concentration of the drug over time. In fact, over time, the drug decreases in the drug-filled core and the polymeric shell, and vice versa, increases in the target tissue.

6   Conclusion

From an analytical and numerical point of view, we analyzed a coupled system of partial differential equations complemented with boundary, interface, and initial conditions. This system can be employed to describe the drug release from a multi-layer capsule into the target tissue where the drug is initially dispersed in the drug-filled core. Since the capsule is surrounded by a polymeric shell, the Fick's law

(a) $P = 2 \times 10^{-8}$

(b) $P = 1 \times 10^{-8}$

(c) $P = 1 \times 10^{-9}$

(d) $P = 1 \times 10^{-10}$
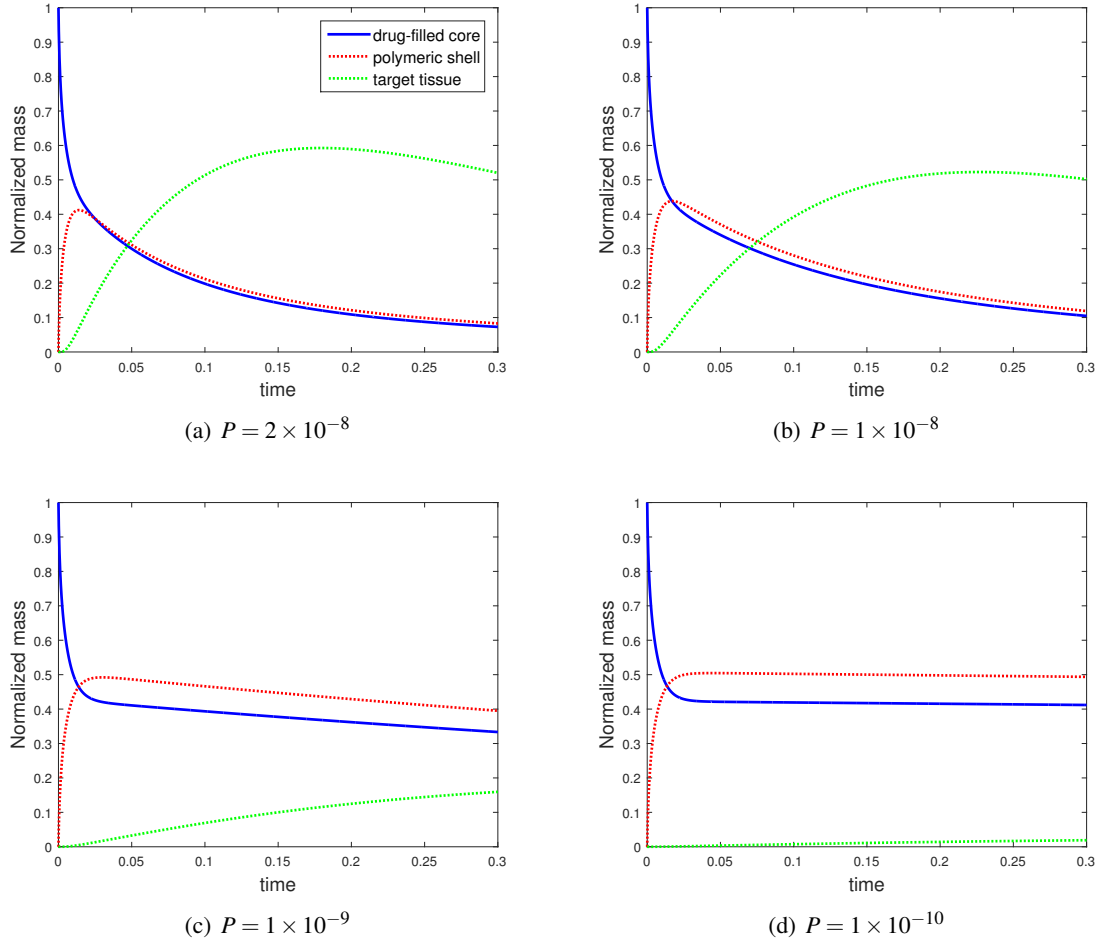
Figure 4: Normalized drug mass profiles in the three layers.

Table 2: Influence of viscoelastic on the drug release

Time	Viscoelastic effect	drug-filled core	polymeric shell	target tissue
0.02	$D_v = 4 \times 10^{-12}$	0.36761253	0.33355918	0.02137680
	$D_v = 4 \times 10^{-10}$	0.36763183	0.33356666	0.02137478
0.1	$D_v = 4 \times 10^{-12}$	0.25443642	0.23476291	0.04375192
	$D_v = 4 \times 10^{-10}$	0.25447180	0.23478178	0.04375025
0.3	$D_v = 4 \times 10^{-12}$	0.10477098	0.09947387	0.04571464
	$D_v = 4 \times 10^{-10}$	0.10480762	0.09949504	0.04571168

is modified through introducing a non-Fickian contribution defined with Maxwell fluid model so as to justify the viscoelastic behavior of the polymeric shell.

We also established the energy estimates of the coupled system. With these estimates, we were able to establish the stability of the system and the uniqueness of the solution.

A numerical method mimicking the continuous model was further suggested. We analyzed the convergence characteristics of the numerical methods, and the numerical results confirmed the convergence results. We ultimately investigated the qualitative behavior of the numerical solutions.

References

[1] E. Azhdari, A. Emami, *Analytical and numerical study of drying of tomato in non-shrinkage and shrinkage model*, Math. Comput. Simul. **166** (2019) 253–265.

[2] E. Azhdari, J.A. Ferreira, P. de Oliveira, P.M. da Silva, *Diffusion, viscoelasticity and erosion: Analytical study and medical applications*, J. Comput. Appl. Math. **275** (2015) 489–501.

[3] S. Barbeiro, J.A. Ferreira, *Coupled vehicle-skin models for drug release*, Comput. Methods Appl. Mech. Eng. **198** (2009) 2078–2086.

[4] H. Brinson, L. Brinson, *Polymer Engineering Science and Viscoelasticity: An Introduction*, Springer, 2008.

[5] E.J. Carr, G. Pontrelli, *Modelling mass diffusion for a multi-layer sphere immersed in a semi-infinite medium: application to drug delivery*, Comput. Biol. Med. **303** (2018) 1–9.

[6] D. Cohen, A.B. White Jr., *Sharp fronts due to diffusion and viscoelastic relaxation in polymers*, SIAM J. Appl. Math. **51** (1991) 472–483.

[7] D.S. Cohen, A.B. White Jr., T.P. Witelski, *Shock Formation in a Multi-Dimensional Viscoelastic Diffusive System*, SIAM J. Appl. Math. **55** (1995) 348–368.

[8] A. Emami, E. Azhdari, J.A. Ferreira, A. Ghaffaripour, *Drying viscoelastic materials: a non-Fickian approach*, Comput. Appl. Math. **39** (2020) 125.

[9] J.A. Ferreira, M. Grassi, E. Gudino, P. de Oliveira, *A 3D model for mechanistic control drug release*, SIAM J. Appl. Math. **74** (2014) 620–633.

[10] J.A. Ferreira, P. de Oliveira, G. Pena, *Transdermal iontophoresisA quantitative and qualitative study*, Comput. Math. Appl. **74** (2017) 2231–2242.

[11] J.A. Ferreira, P. de Oliveira, P. da Silva, *Reaction-diffusion in viscoelastic materials*, J. Comput. Appl. Math. **236** (2012) 3783–3795.

[12] J. Ferreira, P. de Oliveira, P. da Silva, *Analytic and numerics of drug release tracking*, J. Comput. Appl. Math. **236** (2012) 3572–3583.

[13] M. Grassi, G. Lamberti, S. Cascone, G. Grassi, *Mathematical modeling of simultaneous drug release and in vivo absorption*, Int. J. Pharm. **418** (2011) 130–141.

[14] S. Henning, D. Edelhoff, B. Ernst, S. Leick, H. Rehage, D. Suter, *Characterizing permeability and stability of microcapsules for controlled drug delivery by dynamic NMR microscopy*, J. Magn. Reson. **221** (2012) 11–18.

[15] B. Kaoui, *Flow and mass transfer around a core-shell reservoir*, Phys. Rev. E. **95** (2017) 063310.

[16] B. Kaoui, M. Lauricella, G. Pontrelli, *Mechanistic modelling of drug release from multi-layer capsules*, Comput. Biol. Med. **93** (2017) 149–157.

[17] S. De Koker, R. Hoogenboom, B. G. De Geest, *Polymeric multilayer capsules for drug delivery*, Chem. Soc. Rev. **41** (2012) 2867–2884.

[18] G. Pontrelli, E.J. Carr, A. Tiribocchi, S. Succi, *Modelling drug delivery from multiple emulsions*, Phys. Rev. E **102** (2020) 023114.

[19] G. Pontrelli, M. Lauricella, J.A. Ferreira, G. Pena, *Iontophoretic transdermal drug delivery: a multi-layered approach*, Math. Med. Biol. **34** (2016) 559–576.

[20] J. Siepmann, N.A. Peppas, *Modeling of drug release from delivery systems based on hydroxypropyl methylcellulose (HPMC)*, Adv. Drug Deliv. Rev. **48** (2001) 139–157.

[21] A.S. Timin, D.J. Gould, G.B. Sukhorukov, *Multi-layer microcapsules: fresh insights and new applications*, Expert Opin. Drug Deliv. **14** (2017) 583–587.